BELLE-CONF-0201
Parallel Session: 7
ABS688

An Improved Measurement of Mixing-induced CP Violation in the Neutral B Meson System

K. Abe,[9] K. Abe,[44] N. Abe,[47] R. Abe,[30] T. Abe,[45] I. Adachi,[9] Byoung Sup Ahn,[16] H. Aihara,[46] M. Akatsu,[23] M. Asai,[10] Y. Asano,[51] T. Aso,[50] V. Aulchenko,[2] T. Aushev,[13] A. M. Bakich,[41] Y. Ban,[34] E. Banas,[28] S. Banerjee,[42] A. Bay,[19] I. Bedny,[2] P. K. Behera,[52] D. Beiline,[2] I. Bizjak,[14] A. Bondar,[2] A. Bozek,[28] M. Bračko,[21,14] J. Brodzicka,[28] T. E. Browder,[8] B. C. K. Casey,[8] M.-C. Chang,[27] P. Chang,[27] Y. Chao,[27] K.-F. Chen,[27] B. G. Cheon,[40] R. Chistov,[13] S.-K. Choi,[7] Y. Choi,[40] Y. K. Choi,[40] M. Danilov,[13] L. Y. Dong,[11] R. Dowd,[22] J. Dragic,[22] A. Drutskoy,[13] S. Eidelman,[2] V. Eiges,[13] Y. Enari,[23] C. W. Everton,[22] F. Fang,[8] H. Fujii,[9] C. Fukunaga,[48] N. Gabyshev,[9] A. Garmash,[2,9] T. Gershon,[9] B. Golob,[20,14] A. Gordon,[22] K. Gotow,[53] H. Guler,[8] R. Guo,[25] J. Haba,[9] K. Hanagaki,[35] F. Handa,[45] K. Hara,[32] T. Hara,[32] Y. Harada,[30] K. Hashimoto,[32] N. C. Hastings,[22] H. Hayashii,[24] M. Hazumi,[9] E. M. Heenan,[22] I. Higuchi,[45] T. Higuchi,[9] L. Hinz,[19] T. Hirai,[47] T. Hojo,[32] T. Hokuue,[23] Y. Hoshi,[44] K. Hoshina,[49] W.-S. Hou,[27] S.-C. Hsu,[27] H.-C. Huang,[27] T. Igaki,[23] Y. Igarashi,[9] T. Iijima,[23] K. Inami,[23] A. Ishikawa,[23] H. Ishino,[47] R. Itoh,[9] M. Iwamoto,[3] H. Iwasaki,[9] Y. Iwasaki,[9] D. J. Jackson,[32] P. Jalocha,[28] H. K. Jang,[39] M. Jones,[8] R. Kagan,[13] H. Kakuno,[47] J. Kaneko,[47] J. H. Kang,[55] J. S. Kang,[16] P. Kapusta,[28] M. Kataoka,[24] S. U. Kataoka,[24] N. Katayama,[9] H. Kawai,[3] H. Kawai,[46] Y. Kawakami,[23] N. Kawamura,[1] T. Kawasaki,[30] H. Kichimi,[9] D. W. Kim,[40] Heejong Kim,[55] H. J. Kim,[55] H. O. Kim,[40] Hyunwoo Kim,[16] S. K. Kim,[39] T. H. Kim,[55] K. Kinoshita,[5] S. Kobayashi,[37] S. Koishi,[47] K. Korotushenko,[35] S. Korpar,[21,14] P. Križan,[20,14] P. Krokovny,[2] R. Kulasiri,[5] S. Kumar,[33] E. Kurihara,[3] A. Kuzmin,[2] Y.-J. Kwon,[55] J. S. Lange,[6,36] G. Leder,[12] S. H. Lee,[39] J. Li,[38] A. Limosani,[22] D. Liventsev,[13] R.-S. Lu,[27] J. MacNaughton,[12] G. Majumder,[42] F. Mandl,[12] D. Marlow,[35] T. Matsubara,[46] T. Matsuishi,[23] S. Matsumoto,[4] T. Matsumoto,[48] Y. Mikami,[45] W. Mitaroff,[12] K. Miyabayashi,[24] Y. Miyabayashi,[23] H. Miyake,[32] H. Miyata,[30] L. C. Moffitt,[22] G. R. Moloney,[22] G. F. Moorhead,[22] S. Mori,[51] T. Mori,[4] A. Murakami,[37] T. Nagamine,[45] Y. Nagasaka,[10] T. Nakadaira,[46] T. Nakamura,[47] E. Nakano,[31] M. Nakao,[9] H. Nakazawa,[4] J. W. Nam,[40] S. Narita,[45] Z. Natkaniec,[28] K. Neichi,[44] S. Nishida,[17] O. Nitoh,[49] S. Noguchi,[24] T. Nozaki,[9] A. Ofuji,[32] S. Ogawa,[43] F. Ohno,[47] T. Ohshima,[23] Y. Ohshima,[47] T. Okabe,[23] S. Okuno,[15] S. L. Olsen,[8] Y. Onuki,[30] W. Ostrowicz,[28] H. Ozaki,[9] P. Pakhlov,[13] H. Palka,[28] C. W. Park,[16] H. Park,[18] K. S. Park,[40] L. S. Peak,[41] J.-P. Perroud,[19] M. Peters,[8] L. E. Piilonen,[53] E. Prebys,[35] J. L. Rodriguez,[8] F. J. Ronga,[19] N. Root,[2] M. Rozanska,[28] K. Rybicki,[28] J. Ryuko,[32] H. Sagawa,[9] S. Saitoh,[9] Y. Sakai,[9] H. Sakamoto,[17] H. Sakaue,[31] M. Satapathy,[52] A. Satpathy,[9,5] O. Schneider,[19] S. Schrenk,[5] C. Schwanda,[9,12] S. Semenov,[13] K. Senyo,[23] Y. Settai,[4] R. Seuster,[8] M. E. Sevior,[22] H. Shibuya,[43] M. Shimoyama,[24] B. Shwartz,[2] A. Sidorov,[2] V. Sidorov,[2] J. B. Singh,[33] N. Soni,[33] S. Stanič,[51,*] M. Starič,[14] A. Sugi,[23] A. Sugiyama,[23] K. Sumisawa,[9] T. Sumiyoshi,[48] K. Suzuki,[9] S. Suzuki,[54] S. Y. Suzuki,[9] S. K. Swain,[8] T. Takahashi,[31] F. Takasaki,[9] K. Tamai,[9] N. Tamura,[30] J. Tanaka,[46] M. Tanaka,[9] G. N. Taylor,[22] Y. Teramoto,[31] S. Tokuda,[23] M. Tomoto,[9] T. Tomura,[46]

S. N. Tovey,[22] K. Trabelsi,[8] W. Trischuk,[35,†] T. Tsuboyama,[9] T. Tsukamoto,[9] S. Uehara,[9] K. Ueno,[27] Y. Unno,[3] S. Uno,[9] Y. Ushiroda,[9] S. E. Vahsen,[35] G. Varner,[8] K. E. Varvell,[41] C. C. Wang,[27] C. H. Wang,[26] J. G. Wang,[53] M.-Z. Wang,[27] Y. Watanabe,[47] E. Won,[16] B. D. Yabsley,[53] Y. Yamada,[9] A. Yamaguchi,[45] H. Yamamoto,[45] T. Yamanaka,[32] Y. Yamashita,[29] M. Yamauchi,[9] H. Yanai,[30] S. Yanaka,[47] J. Yashima,[9] P. Yeh,[27] M. Yokoyama,[46] K. Yoshida,[23] Y. Yuan,[11] Y. Yusa,[45] H. Yuta,[1] C. C. Zhang,[11] J. Zhang,[51] Z. P. Zhang,[38] Y. Zheng,[8] V. Zhilich,[2] Z. M. Zhu,[34] and D. Žontar[51]

(The Belle Collaboration)

[1]*Aomori University, Aomori*
[2]*Budker Institute of Nuclear Physics, Novosibirsk*
[3]*Chiba University, Chiba*
[4]*Chuo University, Tokyo*
[5]*University of Cincinnati, Cincinnati OH*
[6]*University of Frankfurt, Frankfurt*
[7]*Gyeongsang National University, Chinju*
[8]*University of Hawaii, Honolulu HI*
[9]*High Energy Accelerator Research Organization (KEK), Tsukuba*
[10]*Hiroshima Institute of Technology, Hiroshima*
[11]*Institute of High Energy Physics, Chinese Academy of Sciences, Beijing*
[12]*Institute of High Energy Physics, Vienna*
[13]*Institute for Theoretical and Experimental Physics, Moscow*
[14]*J. Stefan Institute, Ljubljana*
[15]*Kanagawa University, Yokohama*
[16]*Korea University, Seoul*
[17]*Kyoto University, Kyoto*
[18]*Kyungpook National University, Taegu*
[19]*Institut de Physique des Hautes Énergies, Université de Lausanne, Lausanne*
[20]*University of Ljubljana, Ljubljana*
[21]*University of Maribor, Maribor*
[22]*University of Melbourne, Victoria*
[23]*Nagoya University, Nagoya*
[24]*Nara Women's University, Nara*
[25]*National Kaohsiung Normal University, Kaohsiung*
[26]*National Lien-Ho Institute of Technology, Miao Li*
[27]*National Taiwan University, Taipei*
[28]*H. Niewodniczanski Institute of Nuclear Physics, Krakow*
[29]*Nihon Dental College, Niigata*
[30]*Niigata University, Niigata*
[31]*Osaka City University, Osaka*
[32]*Osaka University, Osaka*
[33]*Panjab University, Chandigarh*
[34]*Peking University, Beijing*
[35]*Princeton University, Princeton NJ*
[36]*RIKEN BNL Research Center, Brookhaven NY*
[37]*Saga University, Saga*

[38] University of Science and Technology of China, Hefei
[39] Seoul National University, Seoul
[40] Sungkyunkwan University, Suwon
[41] University of Sydney, Sydney NSW
[42] Tata Institute of Fundamental Research, Bombay
[43] Toho University, Funabashi
[44] Tohoku Gakuin University, Tagajo
[45] Tohoku University, Sendai
[46] University of Tokyo, Tokyo
[47] Tokyo Institute of Technology, Tokyo
[48] Tokyo Metropolitan University, Tokyo
[49] Tokyo University of Agriculture and Technology, Tokyo
[50] Toyama National College of Maritime Technology, Toyama
[51] University of Tsukuba, Tsukuba
[52] Utkal University, Bhubaneswer
[53] Virginia Polytechnic Institute and State University, Blacksburg VA
[54] Yokkaichi University, Yokkaichi
[55] Yonsei University, Seoul
(Dated: February 7, 2008)

Abstract

We present an improved measurement of the standard model CP violation parameter $\sin 2\phi_1$ (also known as $\sin 2\beta$) based on a sample of 85×10^6 $B\overline{B}$ pairs collected at the $\Upsilon(4S)$ resonance with the Belle detector at the KEKB asymmetric-energy e^+e^- collider. One neutral B meson is reconstructed in a $J/\psi K^0_S$, $\psi(2S)K^0_S$, $\chi_{c1}K^0_S$, $\eta_c K^0_S$, $J/\psi K^{*0}$, or $J/\psi K^0_L$ CP-eigenstate decay channel and the flavor of accompanying B meson is identified from its decay products. From the asymmetry in the distribution of the time intervals between the two B meson decay points, we obtain $\sin 2\phi_1 = 0.719 \pm 0.074(\mathrm{stat}) \pm 0.035(\mathrm{syst})$. We also report measurements of CP violation parameters for the related $B^0 \to J/\psi\pi^0$ decay mode and the penguin-dominated processes $B^0 \to \eta' K^0_S$, ϕK^0_S and $K^+K^-K^0_S$.

PACS numbers: 11.30.Er, 12.15.Hh, 13.25.Hw

In the Standard Model (SM), CP violation arises from an irreducible complex phase in the weak interaction quark-mixing matrix (CKM matrix) [1]. In particular, the SM predicts a CP-violating asymmetry in the time-dependent rates for B^0 and $\overline{B}^0$ decays to a common CP eigenstate, f_{CP}, with negligible corrections from strong interactions[2]:

$$A(t) \equiv \frac{\Gamma(\overline{B}^0 \to f_{CP}) - \Gamma(B^0 \to f_{CP})}{\Gamma(\overline{B}^0 \to f_{CP}) + \Gamma(B^0 \to f_{CP})} = -\xi_f \sin 2\phi_1 \sin(\Delta m_d t), \tag{1}$$

where $\Gamma(B^0, \overline{B}^0 \to f_{CP})$ is the decay rate for a B^0 or $\overline{B}^0$ to f_{CP} dominated by a $b \to c\overline{c}s$ transition at a proper time t after production, ξ_f is the CP eigenvalue of f_{CP}, Δm_d is the mass difference between the two B^0 mass eigenstates, and ϕ_1 is one of the three interior angles of the CKM unitarity triangle, defined as $\phi_1 \equiv \pi - \arg(-V_{tb}^* V_{td} / - V_{cb}^* V_{cd})$. Non-zero values for $\sin 2\phi_1$ were reported by the Belle and BaBar groups[3, 4].

Belle's published measurement of $\sin 2\phi_1$ is based on a 29.1 fb^{-1} data sample containing 31.3×10^6 $B\overline{B}$ pairs produced at the $\Upsilon(4S)$ resonance. In this paper, we report an improved measurement that uses 85×10^6 $B\overline{B}$ pairs (78 fb^{-1}). The data were collected with the Belle detector [5] at the KEKB asymmetric collider [6], which collides 8.0 GeV e^- on 3.5 GeV e^+ at a small ($\pm$11 mrad) crossing angle. We use events where one of the B mesons decays to f_{CP} at time t_{CP}, and the other decays to a self-tagging state, $f_{\rm tag}$, *i.e.*, a final state that distinguishes B^0 and $\overline{B}^0$, at time $t_{\rm tag}$. The CP violation manifests itself as an asymmetry $A(\Delta t)$, where Δt is the proper time interval between the two decays: $\Delta t \equiv t_{CP} - t_{\rm tag}$. At KEKB, the $\Upsilon(4S)$ resonance is produced with a boost of $\beta\gamma = 0.425$ nearly along the electron beam direction (z direction), and Δt can be determined as $\Delta t \simeq \Delta z/(\beta\gamma)c$, where Δz is the z distance between the f_{CP} and $f_{\rm tag}$ decay vertices, $\Delta z \equiv z_{CP} - z_{\rm tag}$. The Δz average value is approximately 200 μm.

The Belle detector [5] is a large-solid-angle spectrometer that consists of a silicon vertex detector (SVD), a central drift chamber (CDC), an array of aerogel threshold Čerenkov counters (ACC), time-of-flight scintillation counters (TOF), and an electromagnetic calorimeter comprised of CsI(Tl) crystals (ECL) located inside a superconducting solenoid coil that provides a 1.5 T magnetic field. An iron flux-return located outside of the coil is instrumented to detect K_L^0 mesons and to identify muons (KLM).

We reconstruct B^0 decays to the following CP eigenstates [7]: $J/\psi K_S^0$, $\psi(2S)K_S^0$, $\chi_{c1}K_S^0$, $\eta_c K_S^0$ for $\xi_f = -1$ and $J/\psi K_L^0$ for $\xi_f = +1$. We also use $B^0 \to J/\psi K^{*0}$ decays where $K^{*0} \to K_S^0\pi^0$. Here the final state is a mixture of even and odd CP, depending on the relative orbital angular momentum of the J/ψ and K^{*0}. We find that the final state is primarily $\xi_f = +1$; the $\xi_f = -1$ fraction is $0.19 \pm 0.02({\rm stat}) \pm 0.03({\rm syst})$[8]. For reconstructed $B \to f_{CP}$ candidates other than $J/\psi K_L^0$, we identify B decays using the energy difference $\Delta E \equiv E_B^{\rm cms} - E_{\rm beam}^{\rm cms}$ and the beam-energy constrained mass $M_{\rm bc} \equiv \sqrt{(E_{\rm beam}^{\rm cms})^2 - (p_B^{\rm cms})^2}$, where $E_{\rm beam}^{\rm cms}$ is the beam energy in the center-of-mass system (cms), and $E_B^{\rm cms}$ and $p_B^{\rm cms}$ are the cms energy and momentum of the reconstructed B candidate, respectively. Figure 1 (left) shows the $M_{\rm bc}$ distributions for all B^0 candidates except for $B^0 \to J/\psi K_L^0$ that have ΔE values in the signal region. Table I lists the numbers of observed candidates ($N_{\rm rec}$).

Candidate $B^0 \to J/\psi K_L^0$ decays are selected by requiring ECL and/or KLM hit patterns that are consistent with the presence of a shower induced by a neutral hadron. The centroid of the shower is required to be in a 45° cone centered on the K_L^0 direction that is inferred from two-body decay kinematics and the measured four-momentum of the J/ψ. Figure 1 (right) shows the $p_B^{\rm cms}$ distribution, calculated with the $B^0 \to J/\psi K_L^0$ two-body decay hypothesis. The histograms are the results of a fit to the signal and background distributions. There

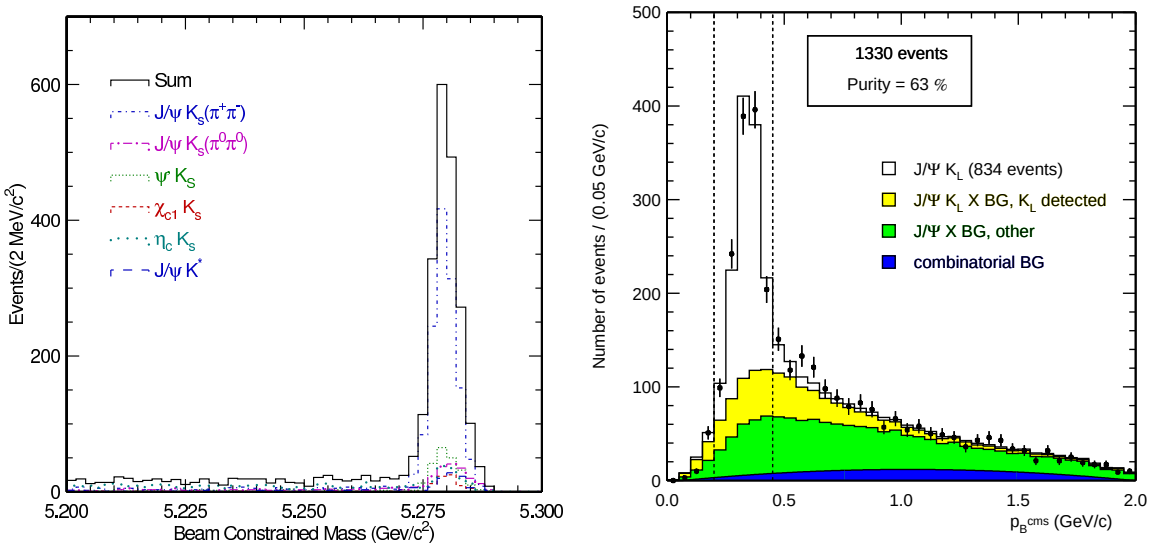

FIG. 1: The beam-energy constrained mass distribution for all decay modes combined other than $J/\psi K_L^0$ (left). The $p_B^{\rm cms}$ distribution for $B^0 \to J/\psi K_L^0$ candidates with the results of the fit (right).

TABLE I: The numbers of reconstructed $B \to f_{CP}$ candidates before flavor tagging and vertex reconstruction ($N_{\rm rec}$), the numbers of events used for the $\sin 2\phi_1$ determination ($N_{\rm ev}$), and the estimated signal purity in the signal region for each f_{CP} mode.

Mode	ξ_f	$N_{\rm rec}$	$N_{\rm ev}$	Purity
$J/\psi(\ell^+\ell^-)K_S^0(\pi^+\pi^-)$	-1	1285	1116	0.98
$J/\psi(\ell^+\ell^-)K_S^0(\pi^0\pi^0)$	-1	188	162	0.82
$\psi(2S)(\ell^+\ell^-)K_S^0(\pi^+\pi^-)$	-1	91	76	0.96
$\psi(2S)(J/\psi\pi^+\pi^-)K_S^0(\pi^+\pi^-)$	-1	112	96	0.91
$\chi_{c1}(J/\psi\gamma)K_S^0(\pi^+\pi^-)$	-1	77	67	0.96
$\eta_c(K_S^0K^-\pi^+)K_S^0(\pi^+\pi^-)$	-1	72	63	0.65
$\eta_c(K^+K^-\pi^0)K_S^0(\pi^+\pi^-)$	-1	49	44	0.72
$\eta_c(p\overline{p})K_S^0(\pi^+\pi^-)$	-1	21	15	0.94
All with $\xi_f = -1$		1895	1639	0.94
$J/\psi(\ell^+\ell^-)K^{*0}(K_S^0\pi^0)$	$-1(19\%)/+1(81\%)$	101	89	0.92
$J/\psi(\ell^+\ell^-)K_L^0$	$+1$	1330	1230	0.63
All		3326	2958	0.81

are 1330 entries in total in the $0.20 \le p_B^{\rm cms} \le 0.45$ GeV/c signal region; the fit indicates a signal purity of 63%. The reconstruction and selection criteria for all of f_{CP} channels used in the measurement are described in more detail elsewhere [3].

Leptons, charged pions, kaons, and Λ baryons that are not associated with a reconstructed CP eigenstate decay are used to identify the b-flavor of the accompanying B meson: high

momentum leptons from $b \to c\ell^-\overline{\nu}$; lower momentum leptons from $c \to s\ell^+\nu$; charged kaons and Λ baryons from $b \to c \to s$; fast pions from $B^0 \to D^{(*)-}(\pi^+, \rho^+, a_1^+$, etc.); and slow pions from $D^{*-} \to \overline{D}^0\pi^-$. Based on the measured properties of these tracks, two parameters, q and r, are assigned to an event. The first, q, has the discrete values $q = \pm 1$ that is $+1$ (-1) when $B_{\rm tag}$ is likely to be a B^0 ($\overline{B}^0$), and the parameter r is an event-by-event Monte-Carlo-determined flavor-tagging dilution factor that ranges from $r = 0$ for no flavor discrimination to $r = 1$ for an unambiguous flavor assignment. It is used only to sort data into six intervals of r, according to flavor purity; the wrong-tag probabilities, w_l ($l = 1, 6$), that are used in the final fit are determined directly from data. Samples of B^0 decays to exclusively reconstructed self-tagged channels are utilized to obtain w_l using time-dependent B^0-$\overline{B}^0$ mixing oscillation: $(N_{\rm OF} - N_{\rm SF})/(N_{\rm OF} + N_{\rm SF}) = (1 - 2w_l)\cos(\Delta m_d \Delta t)$, where $N_{\rm OF}$ and $N_{\rm SF}$ are the numbers of opposite and same flavor events. The event fractions and wrong tag fractions are summarized in Table II. The total effective tagging efficiency is determined to be $\sum_{l=1}^{6} f_l(1 - 2w_l)^2 = 0.288 \pm 0.006$, where f_l is the event fraction for each r interval.

TABLE II: The event fractions (ϵ_l) and wrong tag fractions (w_l) fo each r interval. The errors include both statistical and systematic uncertainties. The event fractions are obtained from the $J/\psi K_S^0$ simulation.

l	r	ϵ_l	w_l
1	0.000 − 0.250	0.399	0.458 ± 0.006
2	0.250 − 0.500	0.146	0.336 ± 0.009
3	0.500 − 0.625	0.104	$0.229\ ^{+0.010}_{-0.011}$
4	0.625 − 0.750	0.122	0.159 ± 0.009
5	0.750 − 0.875	0.094	0.111 ± 0.009
6	0.875 − 1.000	0.137	$0.020\ ^{+0.007}_{-0.006}$

The vertex position for the f_{CP} decay is reconstructed using leptons from J/ψ decays or kaons and pions from η_c and that for $f_{\rm tag}$ is obtained with well reconstructed tracks that are not assigned to f_{CP}. Tracks that are consistent with coming from a $K_S^0 \to \pi^+\pi^-$ decay are not used. Each vertex position is required to be consistent with a run-by-run-determined interaction region profile that is smeared in the r-ϕ plane by the B meson decay length. With these requirements, we are able to determine a vertex even with a single track; the fraction of single-track vertices is about 10% for z_{CP} and 22% for $z_{\rm tag}$. The proper-time interval resolution function, $R_{\rm sig}(\Delta t)$, is formed by convolving four components: the detector resolutions for z_{CP} and $z_{\rm tag}$, the shift in the $z_{\rm tag}$ vertex position due to secondary tracks originating from charmed particle decays, and smearing due to the kinematic approximation used to convert Δz to Δt. A small component of broad outliers in the Δz distribution, caused by mis-reconstruction, is represented by a Gaussian function. We determine twelve resolution parameters from the data from fits to the neutral and charged B meson lifetimes [9] and obtain an average Δt resolution of ~ 1.43 ps (rms). The width of the outlier component is determined to be (42^{+5}_{-4}) ps; the fractional areas are $(2 \pm 1) \times 10^{-4}$ and $(2.7 \pm 0.2) \times 10^{-2}$ for the multiple- and single-track cases, respectively.

After flavor tagging and vertexing, we find 1465 events with $q = +1$ flavor tags and 1493 events with $q = -1$. Table I lists the numbers of candidates used for the $\sin 2\phi_1$ determination ($N_{\rm ev}$) and the estimated signal purity in the signal region for each f_{CP} mode. Figure 2 shows the observed Δt distributions for the $q\xi_f = +1$ (solid points) and $q\xi_f = -1$

(open points) event samples. The asymmetry between the two distributions demonstrates the violation of CP symmetry. We determine $\sin 2\phi_1$ from an unbinned maximum-likelihood

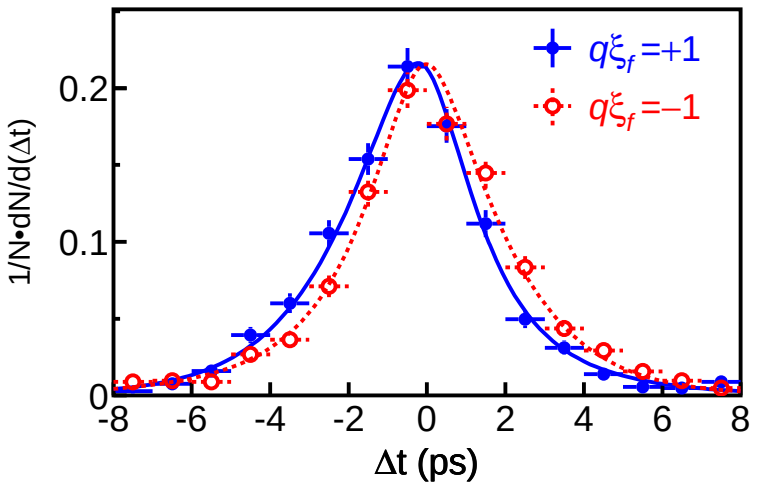

FIG. 2: Δt distributions for the events with $q\xi_f = +1$ (solid points) and $q\xi_f = -1$ (open points). The results of the global fit with $\sin 2\phi_1 = 0.719$ are shown as solid and dashed curves, respectively.

fit to the observed Δt distributions. The probability density function (pdf) expected for the signal distribution is given by

$$\mathcal{P}_{\rm sig}(\Delta t, q, w_l, \xi_f) = \frac{e^{-|\Delta t|/\tau_{B^0}}}{4\tau_{B^0}}[1 - q\xi_f(1-2w_l)\sin 2\phi_1 \sin(\Delta m_d \Delta t)], \qquad (2)$$

where we fix the B^0 lifetime (τ_{B^0}) and mass difference at their world average values[10]. Each pdf is convolved with the appropriate $R_{\rm sig}(\Delta t)$ to determine the likelihood value for each event as a function of $\sin 2\phi_1$:

$$\begin{aligned} P_i \;=\; & (1-f_{\rm ol}) \int \Big[f_{\rm sig}\mathcal{P}_{\rm sig}(\Delta t', q, w_l, \xi_f) R_{\rm sig}(\Delta t - \Delta t') \\ & + (1-f_{\rm sig})\mathcal{P}_{\rm bkg}(\Delta t') R_{\rm bkg}(\Delta t - \Delta t') \Big] d\Delta t' + f_{\rm ol} P_{\rm ol}(\Delta t), \end{aligned} \qquad (3)$$

where $f_{\rm sig}$ is the signal probability calculated as a function of $p_B^{\rm cms}$ for $J/\psi K_L^0$ and of ΔE and $M_{\rm bc}$ for other modes. $\mathcal{P}_{\rm bkg}(\Delta t)$ is the pdf for combinatorial background events, which is modeled as a sum of exponential and prompt components. It is convolved with a sum of two Gaussians, $R_{\rm bkg}$, which is regarded as a resolution function for the background. To account for a small number of events that give large Δt in both the signal and background, we introduce the pdf, $P_{\rm ol}$, and the fractional area, $f_{\rm ol}$, of the outlier component. The only free parameter in the final fit is $\sin 2\phi_1$, which is determined by maximizing the likelihood function $L = \prod_i P_i$, where the product is over all events. The result of the fit is

$$\sin 2\phi_1 = 0.719 \pm 0.074({\rm stat}) \pm 0.035({\rm syst}).$$

The systematic error is dominated by uncertainties in the vertex reconstruction (0.022). Other significant contributions come from uncertainties in: w_l (0.015); the resolution function parameters (0.014); a possible bias in the $\sin 2\phi_1$ fit (0.011); and the $J/\psi K_L^0$ background fraction (0.010). The errors introduced by uncertainties in Δm_d and τ_{B^0} are less than 0.010.

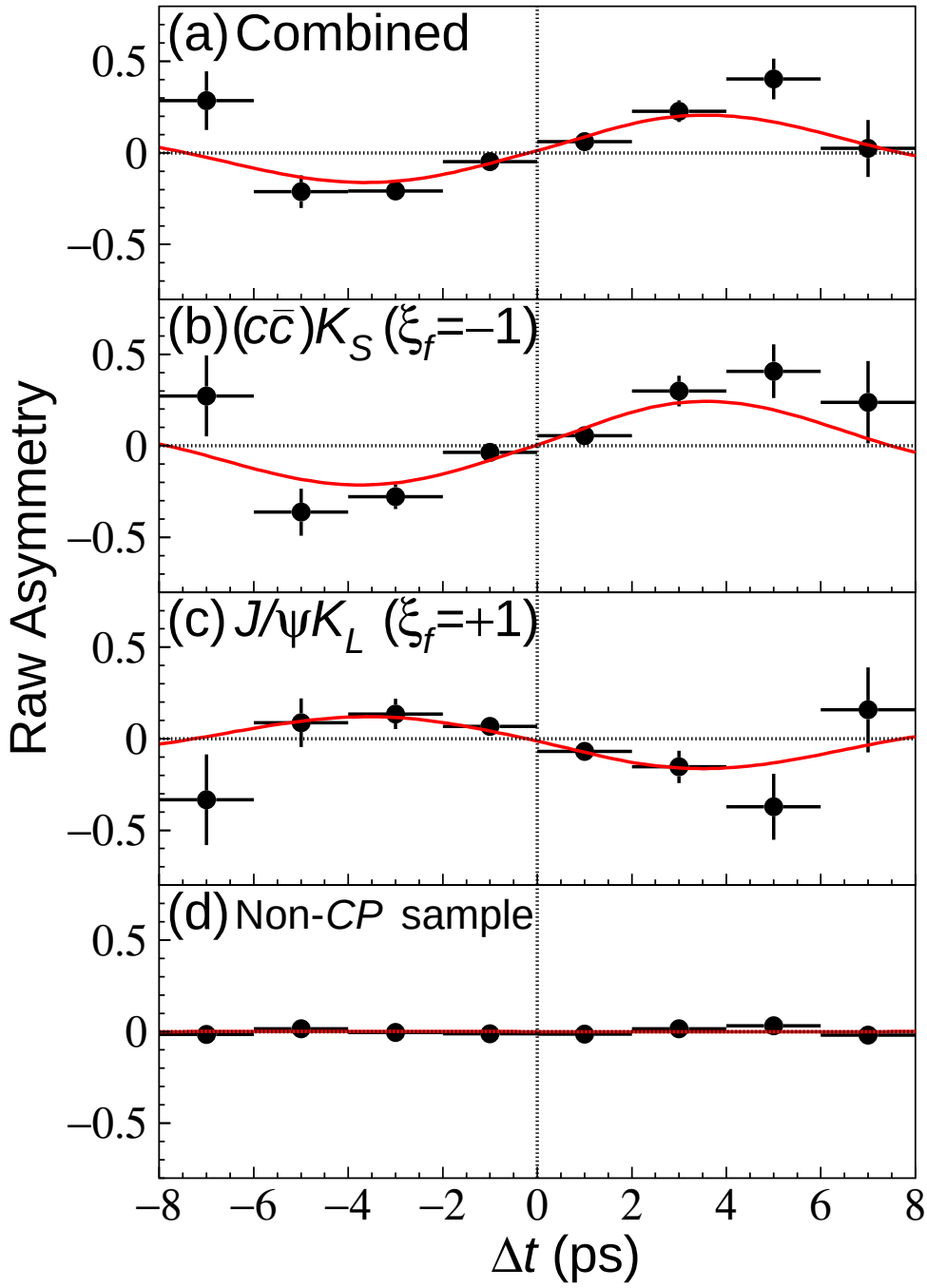

FIG. 3: (a) The raw asymmetry for all modes combined. The asymmetry for $J/\psi K^0_L$ and $J/\psi K^{*0}$ is inverted to account for the opposite CP eigenvalue. The corresponding plots for (b) $(c\bar{c})K^0_S$, (c) $J/\psi K^0_L$, and (d) non-CP control samples are also shown. The curves are the results of the unbinned maximum likelihood fit applied separately to the individual data samples.

TABLE III: The numbers of candidate events ($N_{\rm ev}$) and values of $\sin 2\phi_1$ for various subsamples (statistical errors only).

Sample	$N_{\rm ev}$	$\sin 2\phi_1$
$J/\psi K^0_S(\pi^+\pi^-)$	1116	0.73 ± 0.10
$(c\overline{c})K^0_S$ except $J/\psi K^0_S(\pi^+\pi^-)$	523	0.67 ± 0.17
$J/\psi K^0_L$	1230	0.78 ± 0.17
$J/\psi K^{*0}(K^0_S\pi^0)$	89	0.04 ± 0.63
$f_{\rm tag} = B^0$ $(q = +1)$	1465	0.65 ± 0.12
$f_{\rm tag} = \overline{B}^0$ $(q = -1)$	1493	0.77 ± 0.09
$0 < r \leq 0.5$	1600	1.26 ± 0.36
$0.5 < r \leq 0.75$	658	0.62 ± 0.15
$0.75 < r \leq 1$	700	0.72 ± 0.09
All	2958	0.72 ± 0.07

A number of checks on the measurement are performed. Table III lists the results obtained by applying the same analysis to various subsamples. All values are statistically consistent with each other. Figure 3(a), (b), and (c) show the raw asymmetries and the fit results for all modes combined, $(c\overline{c})K^0_S$, and $J/\psi K^0_L$, respectively. A fit to the non-CP eigenstate self-tagged modes $B^0 \to D^{(*)-}\pi^+$, $D^{*-}\rho^+$, $J/\psi K^{*0}(K^+\pi^-)$, and $D^{*-}\ell^+\nu$, where no asymmetry is expected, yields 0.004 ± 0.015(stat). Figure 3(d) shows the raw asymmetry for these non-CP control samples.

The signal pdf for a neutral B meson decaying into a CP eigenstate (Eq. (2)) can be expressed in a more general form as

$$\mathcal{P}_{\rm sig}(\Delta t, q, w_l, \xi_f) = \frac{e^{-|\Delta t|/\tau_{B^0}}}{4\tau_{B^0}}\Big\{1 + q(1-2w_l)\Big[\frac{2|\lambda|(-\xi_f)a_{CP}}{|\lambda|^2+1}\sin(\Delta m_d \Delta t) + \frac{|\lambda|^2-1}{|\lambda|^2+1}\cos(\Delta m_d \Delta t)\Big]\Big\}, \qquad (4)$$

where λ is a complex parameter that depends on both B^0-$\overline{B}^0$ mixing and on the amplitudes for B^0 and $\overline{B}^0$ decay to a CP eigenstate. The parameter a_{CP} in the coefficient of $\sin(\Delta m_d \Delta t)$ is given by $a_{CP} = -\xi_f Im\lambda/|\lambda|$ and is equal to $\sin 2\phi_1$ in the SM. The presence of the cosine term ($|\lambda| \neq 1$) would indicate direct CP violation; the value for $\sin 2\phi_1$ reported above is determined with the assumption $|\lambda| = 1$, as expected in the SM. In order to test this assumption, we also performed a fit using the above expression with a_{CP} and $|\lambda|$ as free parameters, keeping everything else the same. We obtain

$$|\lambda| = 0.950 \pm 0.049(\text{stat}) \pm 0.026(\text{syst})$$

and $a_{CP} = 0.720 \pm 0.074$(stat) for all CP modes combined, where the sources of the systematic error for $|\lambda|$ are the same as those for $\sin 2\phi_1$. This result confirms the assumption used in our analysis.

Finally, we also report on the time-dependent CP asymmetries in the $B^0 \to \eta' K^0_S$, $B^0 \to \phi K^0_S$ and $B^0 \to K^+K^-K^0_S$ decays that are dominated by the $b \to s$ penguin diagrams, and in the $B^0 \to J/\psi\pi^0$ decay governed by the Cabibbo-suppressed $b \to c\overline{c}d$ transition.

All measurements are based on 85×10^6 $B\overline{B}$ pairs. The reconstruction methods for these modes are described elsewhere [11, 12]. The signal yields are summarized in Table IV. The flavor-tagging, vertexing and fitting techniques are the same as those described above. The decay rate has a time dependence given by

$$\mathcal{P}_{\rm sig}(\Delta t, q, w_l) = \frac{e^{-|\Delta t|/\tau_{B^0}}}{4\tau_{B^0}}\Big\{1 + q(1-2w_l)[\mathcal{S}\sin(\Delta m_d \Delta t) + \mathcal{A}\cos(\Delta m_d \Delta t)]\Big\}. \qquad (5)$$

Table IV summarizes the results of the fits to the Δt distributions. In the table, we show the values of $-\xi_f \mathcal{S}$ denoted by "$\sin 2\phi_1$", since it should be equal to $\sin 2\phi_1$ in the limit that new physics in the penguin loop does not contribute additional CP-violating phases.

TABLE IV: Results of the CP asymmetry parameter measurements for $B^0 \to \eta' K^0_S$, $B^0 \to \phi K^0_S$, $B^0 \to K^+K^-K^0_S$, and $B^0 \to J/\psi\pi^0$ decays. "$\sin 2\phi_1$" is defined as $-\xi_f\mathcal{S}$ and should be equal to $\sin 2\phi_1$ in the limit of no contributions from new physics in the penguin loop. For "$\sin 2\phi_1$" and $\mathcal{A}$, the first errors are statistical and the second errors are systematic. The third errors for the $K^+K^-K^0_S$ mode arise from the uncertainty in the fraction of the CP-odd component [12].

Mode	ξ_f	$N_{\rm ev}$	Purity (%)	"$\sin 2\phi_1$"	$\mathcal{A}$
$\eta' K^0_S$	-1	299	49	$+0.76 \pm 0.36^{+0.05}_{-0.06}$	$+0.26 \pm 0.22 \pm 0.03$
ϕK^0_S	-1	53	67	$-0.73 \pm 0.64 \pm 0.18$	$-0.56 \pm 0.41 \pm 0.12$
$K^+K^-K^0_S$	$-1(3\%)/+1(97\%)$	191	49	$+0.52 \pm 0.46 \pm 0.11^{+0.27}_{-0.03}$	$-0.42 \pm 0.36 \pm 0.09^{+0.03}_{-0.22}$
$J/\psi\pi^0$	$+1$	57	86	$+0.93 \pm 0.49 \pm 0.08$	$-0.25 \pm 0.39 \pm 0.06$

We wish to thank the KEKB accelerator group for the excellent operation of the KEKB accelerator. We acknowledge support from the Ministry of Education, Culture, Sports, Science, and Technology of Japan and the Japan Society for the Promotion of Science; the Australian Research Council and the Australian Department of Industry, Science and Resources; the National Science Foundation of China under contract No. 10175071; the Department of Science and Technology of India; the BK21 program of the Ministry of Education of Korea and the CHEP SRC program of the Korea Science and Engineering Foundation; the Polish State Committee for Scientific Research under contract No. 2P03B 17017; the Ministry of Science and Technology of the Russian Federation; the Ministry of Education, Science and Sport of the Republic of Slovenia; the National Science Council and the Ministry of Education of Taiwan; and the U.S. Department of Energy.

* on leave from Nova Gorica Polytechnic, Nova Gorica
† on leave from University of Toronto, Toronto ON

[1] M. Kobayashi and T. Maskawa, Prog. Theor. Phys. **49**, 652 (1973).
[2] A. B. Carter and A. I. Sanda, Phys. Rev. D **23**, 1567 (1981); I. I. Bigi and A. I. Sanda, Nucl. Phys. **B193**, 85 (1981).
[3] K. Abe *et al.* (Belle Collab.), Phys. Rev. Lett. **87**, 091802 (2001); K. Abe *et al.* (Belle Collab.), hep-ex/0202027, accepted for publication in Phys. Rev. D.
[4] B. Aubert *et al.* (BaBar Collab.), Phys. Rev. Lett. **87**, 091801 (2001); B. Aubert *et al.* (BaBar Collab.), hep-ex/0201020, submitted to Phys. Rev. D.

[5] A. Abashian *et al.* (Belle Collab.), Nucl. Instr. and Meth. A **479**, 117 (2002).
[6] E. Kikutani ed., KEK Preprint 2001-157 (2001), to appear in Nucl. Instr. and Meth. A.
[7] Throughout this paper, when a decay mode is quoted, the inclusion of the charge conjugation mode is implied.
[8] K. Abe *et al.* (Belle Collab.), Phys. Lett. B **538**, 11 (2002).
[9] K. Abe *et al.* (Belle Collab.), Phys. Rev. Lett. **88**, 171801 (2002).
[10] K. Hagiwara *et al.*, Particle Data Group, Phys. Rev. D **66**, 010001 (2002).
[11] K.-F. Chen *et al.* (Belle Collab.), "*Measurement of CP-Violating Parameters in $B \to \eta' K$ Decays*", hep-ex/0207033, to appear in *Phys. Lett. B* (2002); K. Abe *et al.* (Belle Collab.), "*Measurement of Branching Fractions for Charmless B Decays into ϕK and ϕK^**", BELLE-CONF-0232 (2002); K. Abe *et al.* (Belle Collab.), "*Study of $B^0 \to J/\psi\pi^0$, $J/\psi\eta$ and $J/\psi\rho^0(\pi^+\pi^-)$ Decays*", BELLE-CONF-0209 (2002).
[12] K. Abe *et al.* (Belle Collab.), "*Charmless B Decays to Three-kaon Final States*", BELLE-CONF-0225 (2002).